

Article

## Sub-Micrometer Size Structure Fabrication Using a Conductive Polymer

Junji Sone <sup>1,†,\*</sup>, Katsumi Yamada <sup>1,†</sup>, Akihisa Asami <sup>2</sup> and Jun Chen <sup>1</sup>

<sup>1</sup> Faculty of Engineering, Tokyo Polytechnic University, 1583 Iiyama Atsugi, Kanagawa 243-0297, Japan; E-Mails: kyamada@chem.t-kougei.ac.jp (K.Y.); chen@mega.t-kougei.ac.jp (J.C.)

<sup>2</sup> Graduation School of Engineering, Tokyo Polytechnic University, 1583 Iiyama Atsugi, Kanagawa 243-0297, Japan; E-Mail: siegs-welch@docomo.ne.jp

† These authors contributed equally to this work.

\* Author to whom correspondence should be addressed; E-Mail: sone@cs.t-kougei.ac.jp; Tel.: +81-46-242-4111 (ext. 2113); Fax: +81-46-242-3000.

Academic Editor: Cheng Luo

Received: 16 October 2014 / Accepted: 24 December 2014 / Published: 29 December 2014

---

**Abstract:** Stereolithography that uses a femtosecond laser was employed as a method for multiphoton-sensitized polymerization. We studied the stereolithography method, which produces duplicate solid shapes corresponding to the trajectory of the laser focus point and can be used to build a three-dimensional (3D) structure using a conductive polymer. To achieve this, we first considered a suitable polymerization condition for line stereolithography. However, this introduced a problem of irregular polymerization. To overcome this, we constructed a support in the polymerized part using a protein material. This method can stabilize polymerization, but it is not suited for building 3D shapes. Therefore, we considered whether heat accumulation causes the irregular polymerization; consequently, the reduction method of the repetition rate of the femtosecond laser was used to reduce the heating process. This method enabled stabilization and building of a 3D shape using photo-polymerization of a conductive polymer.

**Keywords:** stereolithography; conductive polymer; multi-photon; femto second laser; protein; repetition rate

---

## 1. Introduction

Conductive polymers, such as polypyrrole, polythiophene, polyaniline, and their derivatives, are very useful materials for opto-electronics and nanotechnology. Their applications include molecular wires, semiconductors, display devices, biosensors, and molecular actuators [1]. Many conducting polymers have been prepared mainly by chemical polymerization or electrochemical polymerization. On the other hand, their polymerization and patterning were simultaneously realized by photochemical polymerization. Using photo-polymerization, a two dimensional pattern of conductive materials can be obtained on the substrate [2–4]. Their process resolution was of micrometer order.

In a recent study, multi-photon stereolithography (SL) using a femtosecond laser has been investigated [5–7]. Focused illumination of such a laser limits the multi-photon absorption process to a space narrower than the laser wavelength. In a previous study conducted by our group, we reported two-dimensional patterning [8] and three-dimensional patterning [9] on a substrate as well as three-dimensional photo-polymerization of a conductive polymer (CP) in a transparent Nafion polymer sheet [10]. However, it is difficult to dissolve a Nafion sheet. Further, polymerization is very slow in an aqueous solution, and a long polymerization time leads to irregular and unstable solidification, which leads to difficulties in building complex three-dimensional (3D) shapes with high accuracy [9]. Improvements have been made in the spatial resolution of SL through temperature control of the resin [11]. Moreover, SL in a solid material that is soluble has many advantages for removing non-polymerized area and spatial resolution [12]. Another factor of unstable fabrication is repetition rate of the femtosecond laser. A high repetition rate resulted in the accumulation of heat [13].

CP is a new material for femtosecond SL. Therefore, we examined the SL condition using basic shapes. First, we searched for the optimal line SL condition using an 8 MHz repetition rate of the laser. In this case, we used high speed scanning to avoid irregular polymerization, but stabilization of the polymerization was difficult in achieving the designed thickness. We tried to achieve high accuracy of the 3D shape by considering a support material. Consequently, we used a soluble protein film (an aqueous solid) that includes the CP, a catalyst and gelatine. In this case, we could stabilize the solidification by repeatedly drawing each trajectory. However, we could not improve the height accuracy of the SL parts. Finally, we deemed that heat accumulation was the reason for the irregular polymerization. Thus, we searched for a more suitable condition of 3D SL by varying the scan speed, number of trajectory repeats and the repetition rate of the laser. Next, we realized the SL condition that produces similar height SL parts as designed shapes. In addition, we considered a shrinkage compensation method for the top layer. Furthermore, we considered the use of our SL parts for metamaterial [14] and so on.

## 2. Experimental Methods

### 2.1. Aqueous Solution

An aqueous solution was used as the polymerization solution that contains 0.1 mM of lithium tetrafluoroborate, 0.2 M of pyrrole, 1 mM of methylviologen, and 1 mM of Ru(bpy)<sub>3</sub><sup>2+</sup>. The Glass with Au electrode was immersed in the polymerization solution.

### 2.2. Stereolithography System

Figure 1 shows construction of SL system. Excitation was provided by a mode-locked Ti/sapphire laser. The repetition rate was 8 MHz and wavelength is 850 nm. The laser pulses have a pulse width of 150 fs with a repetition rate of 80 MHz. The laser beam was tightly focused by a water immersion objective lens (NA = 0.95, Nikon Plan Apo 100×, Nikon, Tokyo, Japan). The illuminated areas were transferred under computer-control by shuttering the beam and driving the substrate using XYZ stage.

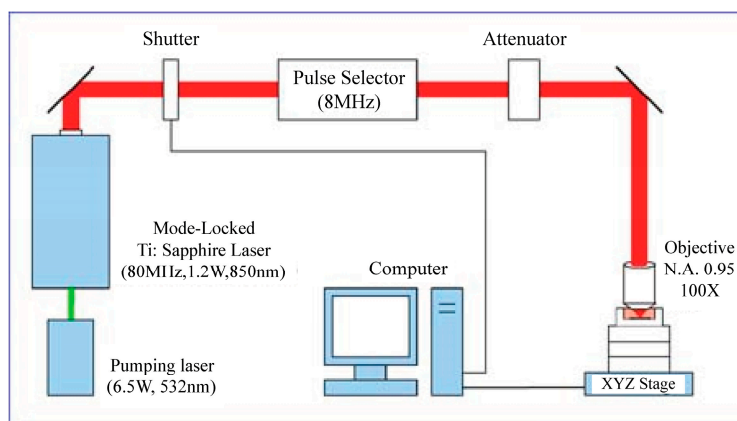


Figure 1. Stereolithography system.

### 2.3. Fabrication Method

#### 2.3.1. Line SL

We searched line SL optimal condition before make a three dimensional structure. Repetition rate of femtosecond laser is 8 MHz. Figure 2 shows the trajectory of the line SL. The first layer was three lines with a horizontal interval pitch  $X_p$  and a second layer consisting of two lines with a horizontal interval pitch  $X_p$  and height interval pitch  $Z_p$ . We used a high scanning speed of 2–8  $\mu\text{m/s}$  to avoid irregular polymerization. Moreover, we tried drawing five times on each trajectory to produce a thick polymerization shape.

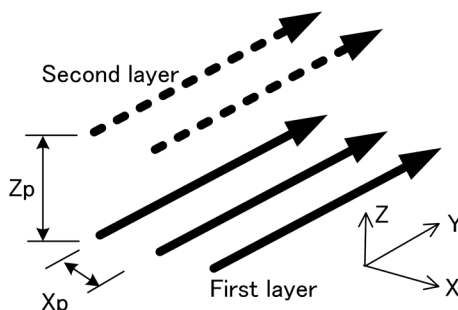


Figure 2. Trajectory of Line stereolithography (SL).

#### 2.3.2. Support Method

To stabilize the irregular polymerization, we used the dissolve support, which can clear away after SL experiment. Note that the SL method necessitates supporting structures under overhanging parts.

Although constructing such supports is feasible using micro SL, it is very difficult to eliminate these parts afterwards. We thus considered that using a dissolvable support would mean we could break up the supports easily after the SL experiment concluded. Then, we considered two methods. In the first method, we used a 20- $\mu\text{m}$  collagen film that included an aqueous solution. The setup is shown in Figure 3a.

In the second method, we added 2% gelatine by weight to the aqueous solution and cooled the mixture to 10 °C for 30 min to achieve solidification. After the SL experiment, the SL part was washed using 40 °C deionized water to dissolve the exception of the SL part. The setup for the SL system is shown in Figure 3b. In this system, the temperature of the aqueous solid was controlled at 10 °C using a thermoelectric module. In the following contents, we described this method as support case.

Figure 2 shows the trajectory of the line SL. The first layer was three lines with a horizontal interval pitch  $X_p$  and a second layer consisting of two lines with a horizontal interval pitch  $X_p$  and height interval pitch  $Z_p$ .

We confirmed three dimensional SL using simple trajectory. Figure 4 shows the 3D SL trajectory. The first layer has three lines with a horizontal interval pitch,  $X_p$ . The second layer has two lines with a horizontal interval pitch  $Y_p$  and height interval pitch of  $Z_p$ . Each path was scanned 15 times, with a scanning speed of 8  $\mu\text{m/s}$  and a laser power of 15 mW.

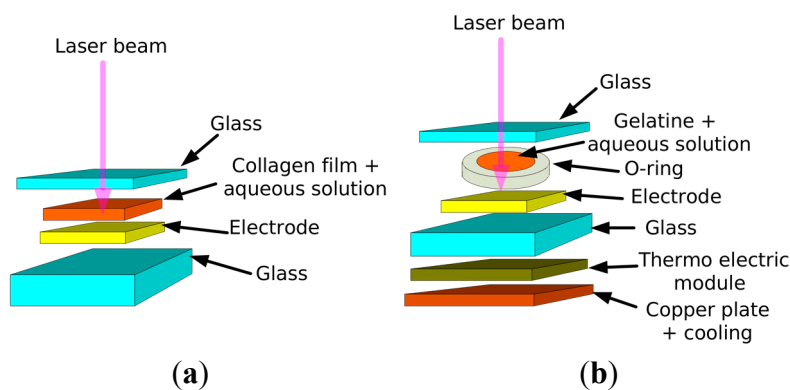


Figure 3. Setting protein film method in SL: (a) Collagen film and (b) gelatine.

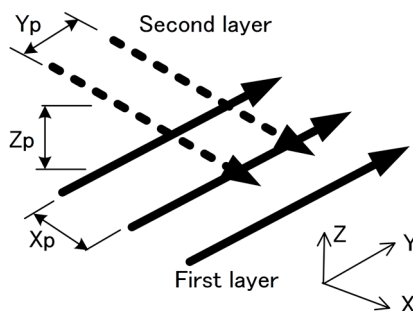


Figure 4. 3D stereolithography (SL) trajectory.

### 2.3.3. Reduction of the Repetition Rate of a Laser

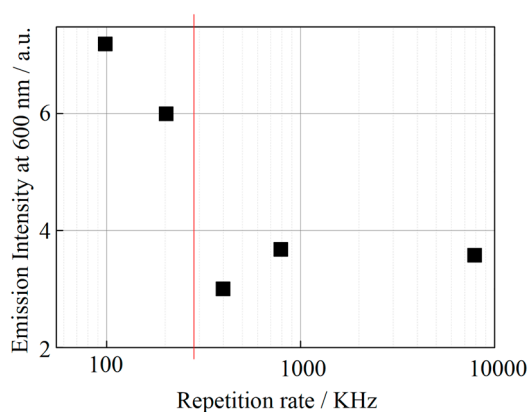
To produce a higher accuracy construction with SL, another method was employed. When the laser repetition rate of a femtosecond laser is high, heat build-up is added to the two-photon polymerization. As a result, the polymerization process was slow (compared with [15]), and the accumulation effect

caused by the heating process was high. Thus, we concluded that the heating process produced the irregular polymerization. Hence, the repetition rate of the laser was reduced.

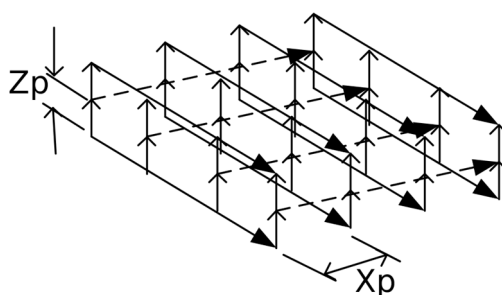
A Pulse picker was used; the pulse energy was lower due to the reduction in the repetition rate. To confirm this assumption, an emission spectrum with the peak near the wavelength of 600 nm (orange color) was visually observed by focusing the femtosecond laser (ex. 850 nm) into the Nafion sheet containing  $\text{Ru}(\text{bpy})_3^{2+}$ . The emission indicated the radiative relaxation of the metal complex from the excited state to the ground state. Figure 5 shows the relationship between the emission intensity at the wavelength of 600 nm and the repetition rate of the laser. The incident laser power was a constant value of 0.28 mW for each repetition rate using a polarizer attenuator. The emission intensities at 100 and 200 kHz were clearly higher than those at 400 kHz to 8 MHz. These results suggested that the radiative relaxation process was depressed at the higher repetition rates by the nonradiative thermal process due to the over-excitation.

Figure 6 shows the trajectory of the 3D SL, constructed using three layers. Each layer has four lines; the first and second lines as well as the second and third lines are orthogonal. Vertical lines were set at intersections. The horizontal interval pitch  $X_p$  was  $1.75 \mu\text{m}$  and the vertical interval pitch,  $Z_p$  was  $0.4 \mu\text{m}$ . The height of the third layer was  $0.8 \mu\text{m}$ .

Abnormal small whiskers are generated by slow scanning speed. Then scan speed is a key factor of SL. Two methods were used to find the optimal scanning method. The first method involved drawing one time on each trajectory and the second method involved drawing six times, repeatedly on each trajectory. Both methods took almost the same laser power in one trajectory. The draw speed of the second method was six times higher than in the first method.



**Figure 5.** Relationships between repetition rate and emission intensity of  $\text{Ru}(\text{bpy})_3^{2+}$  in the Nafion sheet [16].



**Figure 6.** Trajectory of fabrication.

### 3. Results

#### 3.1. Line SL

Figure 7 shows the SEM photograph of the line SL result. We used the trajectory of fabrication in Figure 2. Each path was scanned one time and the laser power was 15 mW. We set  $X_p$  at 0.3, 0.5, 0.7, 0.9  $\mu\text{m}$ .  $Z_p$  was 0.3, 0.6  $\mu\text{m}$  and the scan speed was 2, 4, 8  $\mu\text{m/s}$ . (a) In the case of a one-time repeat, small abnormal whiskers were visible at a low speed of 2–4  $\mu\text{m/s}$ . (b) Each path was repeated five times with a laser power of 15 mW. The width of the SL part obviously changed with the variation in the horizontal interval pitch,  $X_p$ . We observed a small abnormal whisker in all cases. From these results, it is difficult to build thick polymerized parts without avoiding irregular polymerization.

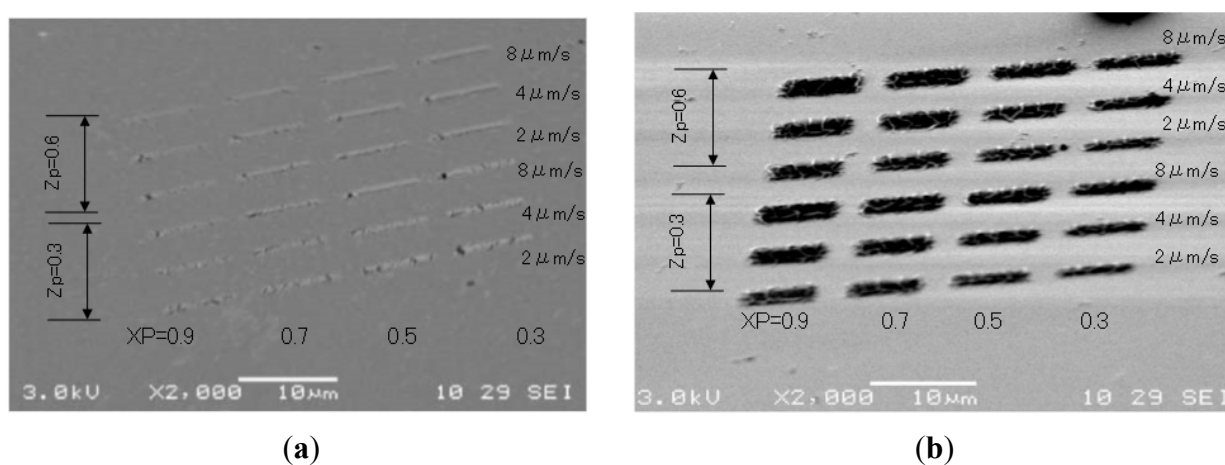


**Figure 7.** Line stereolithography (SL) result: (a) Case of one time repeat and (b) case of fine times repeat.

#### 3.2. Support Method

##### 3.2.1. Case of Collagen Film

Figure 8 shows the results of the SL lines using collagen film that included an aqueous solution, with a laser power of 30 mW and scan speeds as shown in figure. The edge-of-line was indistinct, the velocity of the SL process was still slow and it was very difficult to handle 20- $\mu\text{m}$  film without wrinkles.

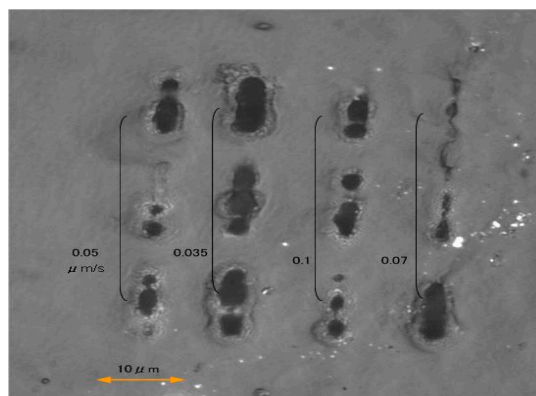


**Figure 8.** Line stereolithography (SL) result in collagen film.

3.2.2. Case of Gelatine

(1) Case of line SL. Figure 9 shows the SEM photograph of the SL result. We used the trajectory of fabrication in Figure 2. Each path was scanned one time and the laser power was 15 mW. We set  $X_p$  at 0.3, 0.5, 0.7, and 0.9  $\mu\text{m}$ .  $Z_p$  was 0.3, 0.6  $\mu\text{m}$  and the scan speed was 2, 4, and 8  $\mu\text{m/s}$ . (a) In the case of a one-time repeat, although the fabricated part was stable with no whisker, the thickness of the polymerized part was lower than the trajectory. (b) Each path was repeated five times with a laser power of 15 mW. The SL part was stable with no whisker. The width of the SL part did not show an obvious change with variations in the horizontal interval pitch,  $X_p$ . In this method, irregular polymerization was inhibited, and we inferred that the laser power was absorbed in the gelatine and the outer part was slightly dissolved by the warm deionized water.

(2) Case of 3D SL. Figure 10 shows the SEM photograph of the SL result with a support case. We used the trajectory of fabrication in Figure 4. We set  $X_p$  at 3  $\mu\text{m}$  and  $Y_p$  at 6  $\mu\text{m}$ . Scanning 15 times is the limit of stable SL. The height was changed following a change in  $Z_p$  from 1.0 to 1.6 and 2.0  $\mu\text{m}$ . The  $Z_p$  case was 3.2  $\mu\text{m}$ , the height of the polymerized material was not changed from that of the case with a  $Z_p$  of 2.0  $\mu\text{m}$ .

Using a gelatine support case, solidification was stabilized; however, multiple repeats of each trajectory to build the designed shape and the precision of the SL shape were not enough to produce a high accuracy construction using sub-micrometre width lines.

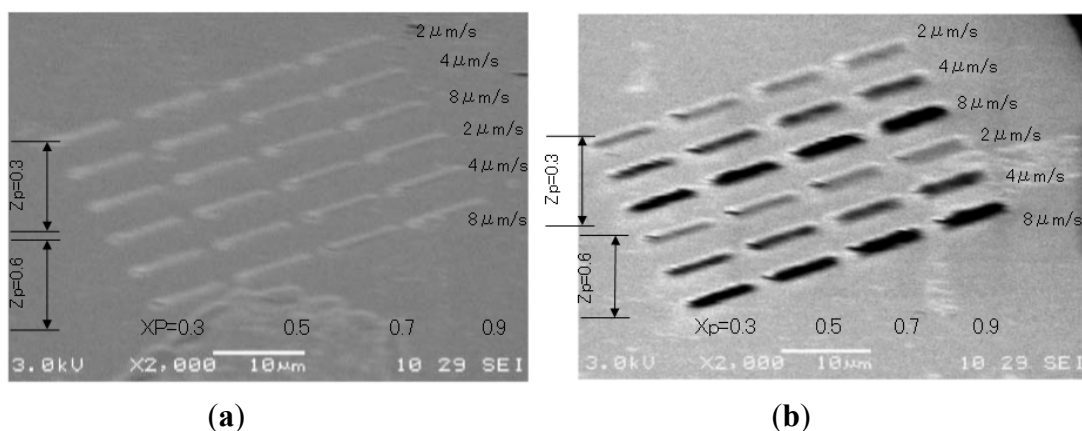


**Figure 9.** Line stereolithography (SL) result for support case: (a) Case of one time repeat and (b) case of fine times repeat.

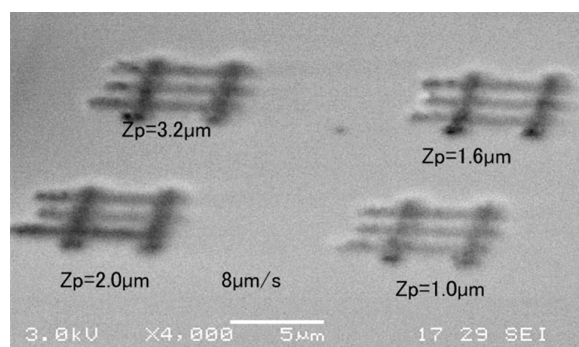


**Figure 10.** 3D stereolithography (SL) result with support case (repeated 15 times).

### 3.3. Reduction of the Repetition Rate of a Laser

#### 3.3.1. First Method (Single Repeat)

To confirm heat accumulation, we tried SL experiments using a slow scan speed and a high repetition rate. Figure 11 shows the SL result when the repetition rate of the femtosecond laser was fixed at 8 MHz and the laser power was varied from 12 to 3 mW. We used the trajectory of fabrication in Figure 6 and repeated once on each trajectory. The scan speed of the left part was  $0.33 \mu\text{m/s}$  and that of the right part was  $0.29 \mu\text{m/s}$ . The solidification part using 12 to 9 mW of laser power was not stable. The laser power was higher for solidification. Although 3 mW was stable, the height of solidification was less than  $0.5 \mu\text{m}$ . The three dimensional fabrication was difficult using this repetition rate.

Figure 12 shows the results of fabrication by reducing the repetition rate from 800 kHz to 20 kHz. The trajectory used is shown in Figure 6 and repeated once on each trajectory. The left scan speed was  $0.29 \mu\text{m/s}$  and the right speed was  $0.33 \mu\text{m/s}$ . The laser powers were 800 kHz: 0.3 mW, 400 kHz: 0.15 mW, 200 kHz: 0.075 mW, 100 kHz: 0.0375 mW, 50 kHz: 0.01875 mW and 20 kHz: 0.00075 mW. The solidification using 800 to 200 kHz was not stable; however, using 50 to 20 kHz was stable. The solidification height was maintained at 1 to 1.5  $\mu\text{m}$ .

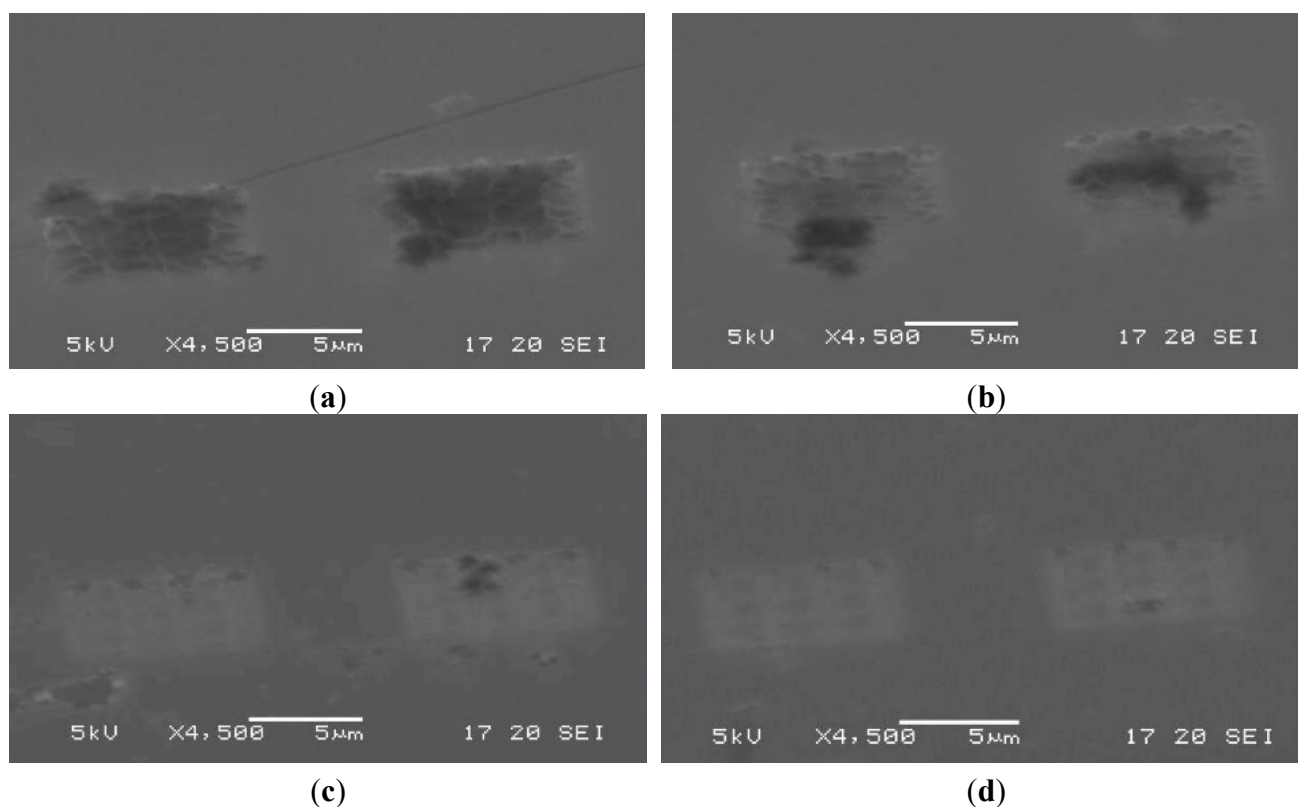


**Figure 11.** Stereolithography (SL) result when the repetition rate was 8 MHz, with variation in laser power. (a) Laser power is 12 mW. (b) Laser power is 9mW. (c) Laser power is 6 mW. (d) Laser power is 3 mW.

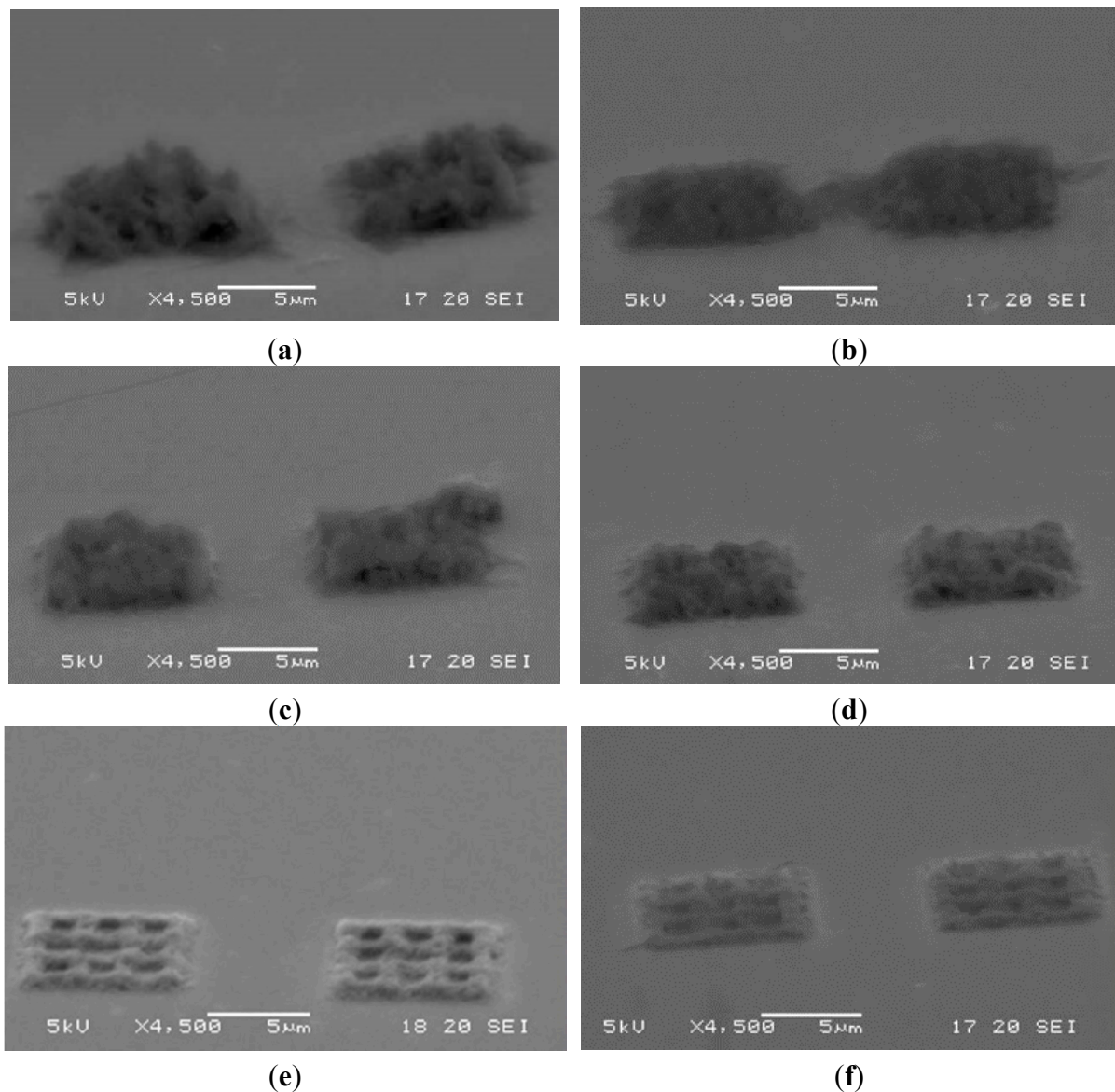


**Figure 12.** Stereolithography (SL) result of reducing the repetition rate from 800 kHz to 20 kHz: (a) 800 kHz, (b) 400 kHz, (c) 200 kHz, (d) 100 kHz, (e) 50 kHz and (f) 20 kHz.

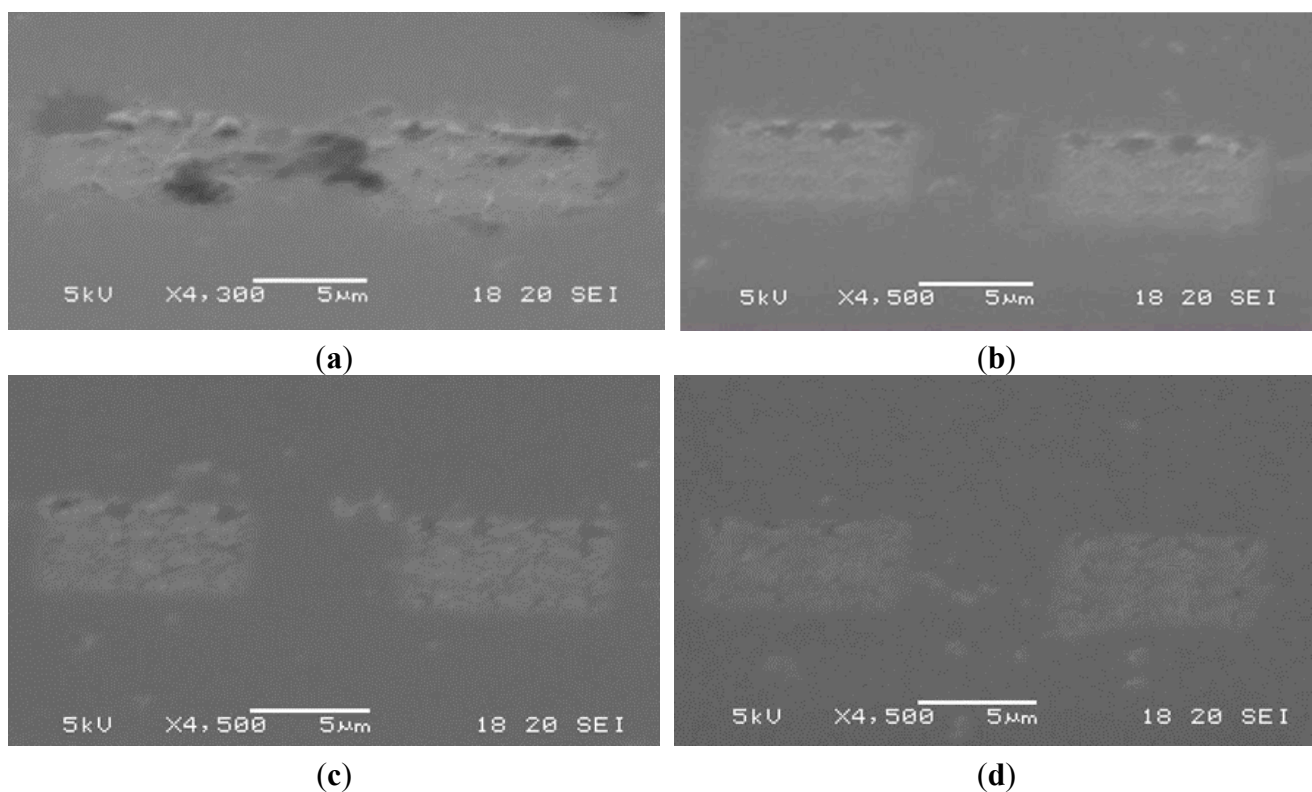
### 3.3.2. Second Method (Six Repeats)

Figure 13 shows the SL result of the repetition rate of a femtosecond laser, fixed to 8 MHz. The laser power was varied from 12 to 3 mW. We used the trajectory of fabrication shown in Figure 6 and this was repeated six times on each trajectory. The left scan speed was 1.54 μm/s and the right speed was 2.0 μm/s. This scan speed was adjusted to the equivalent power, repeating each trajectory once. Solidification using 12 to 9 mW laser power was not stable, which indicates that higher laser power was higher for solidification. Although 3 mW was stable in (a) to (d), the height of solidification is less than 0.5 μm. Three dimensional fabrication is difficult using this repetition rate.

Figure 14 shows the fabrication result by reducing the repetition rate from 800 to 20 kHz. The trajectory used is shown in Figure 6 and repeated six times for each trajectory. The left scan speed was 1.54 μm/s and the right scan speed was 2.0 μm/s. Solidification using 800 kHz to 200 kHz was not stable; however, solidification using 100 to 50 kHz was stable and the solidification height was maintained at 1 to 1.5 μm.

Therefore, we confirmed that the reduction of the repetition rate of the femtosecond laser can stabilize the SL and this method can use three dimensional SL. At 100 kHz, scanning method with drawing six times is stable than drawing one time.

Figure 15 shows the relation between shape magnification and repetition rate of the laser. We used a base height of 1  $\mu\text{m}$  because the highest trajectory is 0.8  $\mu\text{m}$  and the height of one line is 0.4  $\mu\text{m}$ . Shape magnification is calculated by dividing the highest dimension by the base height for each SL result. Abnormal solidification is reduced by decreasing the repetition rate to below 100 kHz. The scanning method of repeating each trajectory six times was a little less stable than a one-time pass. We infer that SL includes sputtering phenomena at 8 MHz.



**Figure 13.** Stereolithography (SL) result when the repetition rate was 8 MHz, with variation in laser power: (a) Laser power is 12 mW, (b) laser power is 9 mW, (c) laser power is 6 mW and (d) laser power is 3 mW.

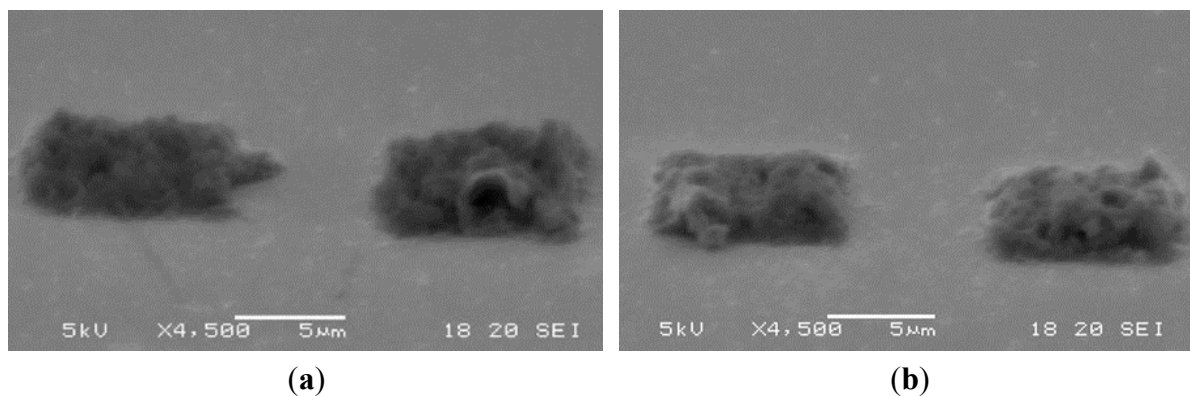


**Figure 14.** Cont.

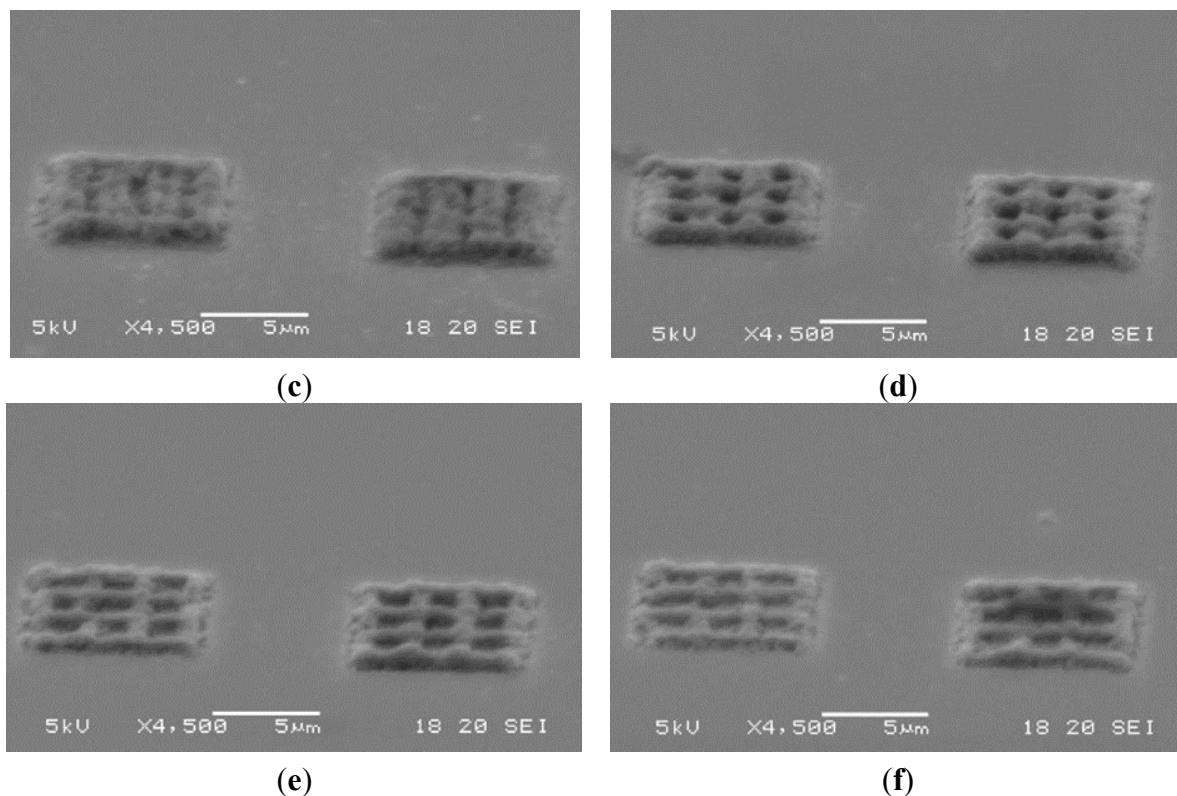


**Figure 14.** Stereolithography (SL) result of reducing the repetition rate from 800 kHz to 20 kHz: (a) 800 kHz, (b) 400 kHz, (c) 200 kHz, (d) 100 kHz, (e) 50 kHz and (f) 20 kHz.

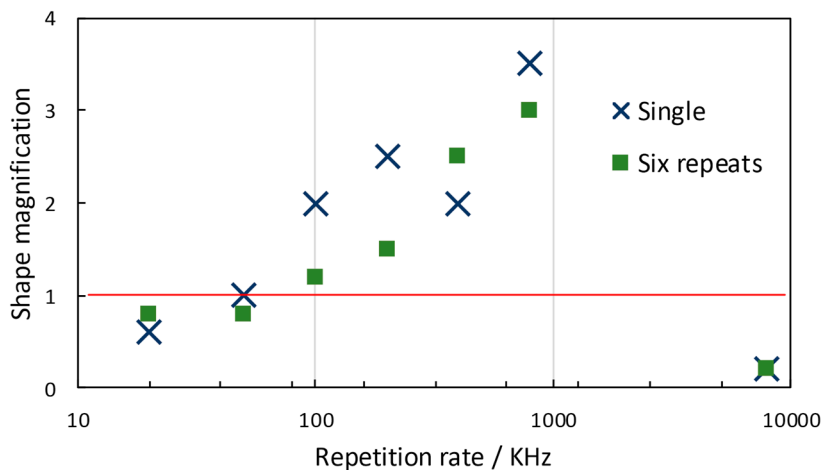
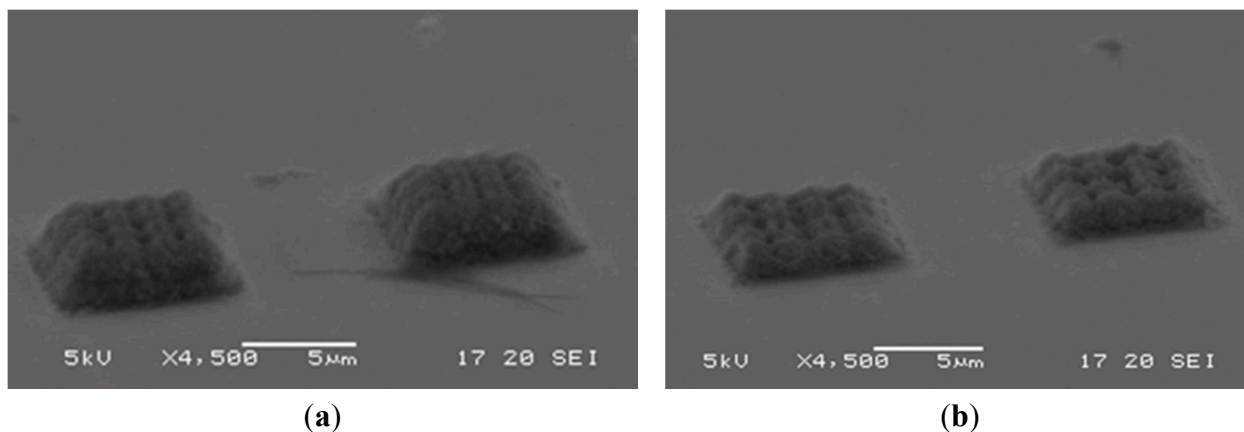


**Figure 15.** Shape accuracy result with changing repetition rate.

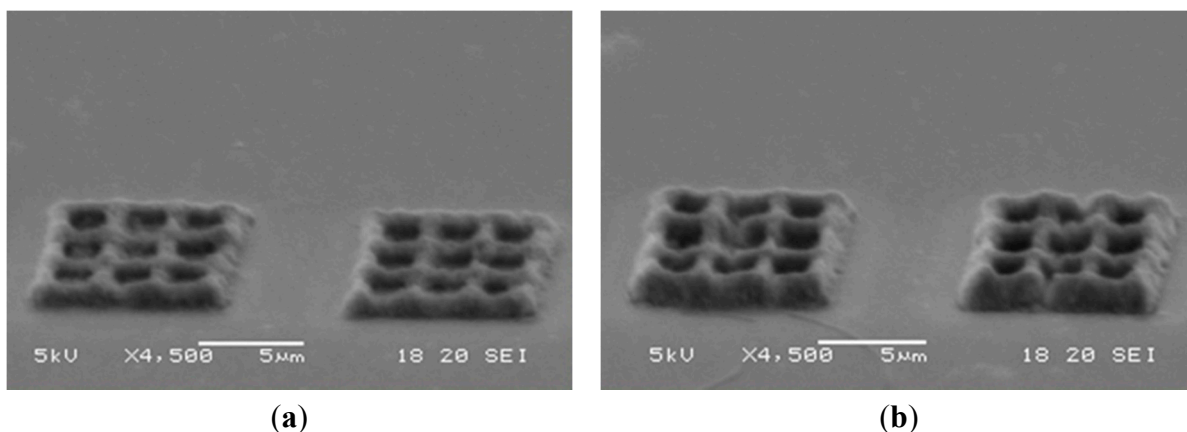
### 3.3.3. Compensation Method of Shrinkage

Figure 16 shows the SL result of nine layers: Figure 16a is one repeat of each trajectory, with a laser repetition rate of 50 kHz and other SL conditions are the same as in Section 3.2.1. Figure 16b is six repetitions of each trajectory, with a laser repetition rate of 50 kHz and other SL conditions are the same as in Section 3.2.2. The top trajectory height was 3.2 μm. In both cases, the SL part has shrinkage around the top layer. In this study, we considered the shrinkage compensation method. The second to nine layer trajectory is expanded 20% at the center from the first trajectory. Figure 17 shows the results of the shrinkage compensation. We reduced the shrinkage at the top layer. These results show that the photo

fabrication can be stabilized by reducing the repetition rate and constructing a three dimensional shape almost similar to this trajectory. This indicates that the resolution for each trajectory needs to be improved in order to build functional NEMS. In the previous study, the polymerization area was ellipsoidal with a depth that was almost five times greater than the horizontal length [17]. We need to solve these problems to achieve high accuracy.



**Figure 16.** Nine layer stereolithography (SL) result. (a) One time for each trajectory, 50 kHz. (b) Six time for each trajectory, 50 kHz.



**Figure 17.** Shrinkage compensation result. (a) One time for each trajectory, 50 kHz. (b) Six time for each trajectory, 50 kHz.

#### 4. Conclusions

In this study, we determined optimal conditions and a suitable method of multiphoton stereolithography using a conductive polymer. First, we tried a high scan speed and multiple repeats on each trajectory using the original aqueous solution and an 8 MHz repetition rate for the laser. However, irregular polymerization was produced when trying to build the designed thickness of the polymerized part. To avoid the irregular polymerization, we used a soluble support. Two percent gelatin by weight was added to the aqueous solution to compose the support for the solidified material. Although this method can reduce irregular polymerization, it required many repeats of each trajectory to build the designed shape and the accuracy of the detail was reduced. Finally, we tried to solve irregular polymerization caused by heat accumulation. We reduced the repetition rate of the femtosecond laser. A

repetition rate of 50–100 kHz was stable for our system and the CP. In addition, we were able to produce a 3D structure with almost the same height as the designed trajectory by utilizing a compensation method for shrinkage during polymerization.

Photo fabrication is stabilized by the reduction of the repetition rate. This SL method can be used to build several micrometer sized three dimensional actuators with micrometer resolution. This method is not archived sub-micrometer resolution, then it is difficult to build high efficiency metamaterials. Further research should be done to find more applications for micrometer/sub-micrometer size three-dimensional conductive polymers.

### Author Contributions

Junji Sone designed the experimental methodologies and made the SL trajectory. Katsumi Yamada developed chemical reaction of electro conductive polymer and measured emission intensity. Akihisa Asami executed the experiments. Jun Chen supported laser optical system.

### Conflicts of Interest

The authors declare no conflict of interest.

### References

1. Kobayashi, N.; Yamada, K.; Hirohashi, R. Effect of Anion Species on Electrochemical Behavior of Poly(aniline)s Electropolymerized in Dichloroethane Solution. *Electrochim. Acta* **1992**, *37*, 2101–2102.
2. Okano, M.; Itoh, K.; Fujishima, A.; Honda, K. Generation of organic conducting patterns on semiconductors by photoelectrochemical polymerization of pyrrole. *Chem. Lett.* **1986**, *15*, 469–472.
3. Iyoda, T.; Toyoda, H.; Fujitsuka, M.; Nakahara, R.; Tsuchiya, H.; Honda, K.; Shimidzu, T. The 100-Å-order depth profile control of polypyrrole-poly(3-methylthiophene) composite thin film by potential-programmed electropolymerization. *J. Phys. Chem.* **1991**, *95*, 5215–5220.
4. Teshima, K.; Yamada, K.; Kobayashi, N.; Hirohashi, R. Photopolymerization of aniline with a tris(2,2'-bipyridyl)ruthenium complex—Methylviologen polymer bilayer electrode system. *Chem. Commun.* **1996**, *1996*, 829–830.
5. Cumpston, B.H.; Ananthavel, S.P.; Barlow, S.; Dyer, D.L.; Ehrlich, J.E.; Erskine, L.L.; Heikal, A.A.; Kuebler, S.M.; Sandy Lee, I.-Y.; McCord-Maughon, D.; Qin, J.; Röckel, H.; Rumi, M.; Wu, X.L.; Marder, S.R.; Perry, J.W. Two-photon polymerization initiators for three-dimensional optical data storage and microfabrication. *Nature* **1999**, *398*, 51–54.
6. Kawata, S.; Sun, H.-B.; Tanaka, T.; Takada, K. Finer Features for Functional Microdevices. *Nature* **2001**, *412*, 697–698.
7. Li, L.; Fourkas, J. Multiphoton Polymerization. *Mater. Today* **2007**, *10*, 30–37.
8. Yamada, K.; Kimura, Y.; Suzuki, S.; Chen, J.; Sone, J. Multiphoton-sensitized polymerization of pyrrole. *Chem. Lett.* **2006**, *35*, 908–909.
9. Sone, J.; Asami, A.; Kimura, G.; Yamada, K. Feasibility study of micro-actuator using electro conducting polymers. *IEEJ Trans. Sens. Micromach.* **2009**, *129*, 81–82.

10. Yamada, K.; Sone, J.; Chen, J. Three-Dimensional Photochemical Microfabrication of Conductive Polymers in Transparent Polymer Sheet. *Opt. Rev.* **2009**, *16*, 208–212.
11. Takada, K.; Kaneko, K.; Li, Y.; Kawata, S.; Chen, Q.; Sun, H. Temperature effects on pinpoint photopolymerization and polymerized micronanostructures. *Appl. Phys. Lett.* **2008**, *92*, 041902.
12. Juodkazis, S.; Mizeikis, V.; Seet, K.; Miwa, M.; Misawa, H. Two-photon lithography of nanorods in SU-8 photoresist. *Nanotechnology* **2005**, *16*, 846–849.
13. Eaton, S.; Zhang, H.; Herman, P.; Yoshino, F.; Shah, L.; Bovatsek, J.; Arai, A. Heat accumulation effects in femtosecond laserwritten waveguides with variable repetition rate. *Opt. Express* **2005**, *13*, 4708–4716.
14. Tanaka, T. Plasmonic metamaterials produced by two-photon-induced photoreduction technique. *J. Laser Micro/Nanoeng.* **2008**, *3*, 152–156.
15. Sun, H.; Kawata, S. Two-Photon Photopolymerization and 3D Lithographic Microfabrication. *NMR 3D Anal. Photopolym.* **2004**, *170*, 169–273.
16. Yamada, K.; Watanabe, M.; Sone, J. Three-Dimensional Printing of Conducting Polymer Microstructures into Transparent Polymer Sheet: Relationship between Process Resolution and Illumination Conditions. *Opt. Rev.* **2014**, *21*, 679–682.
17. Yamada, K.; Kyoya, A.; Sone, J.; Chen, J. Evaluations of Vertical Resolution of Conductive Polymer Three-Dimensional Microstructures Photofabricated in Transparent Polymer Sheet. *Opt. Rev.* **2011**, *18*, 162–165.

© 2014 by the authors; licensee MDPI, Basel, Switzerland. This article is an open access article distributed under the terms and conditions of the Creative Commons Attribution license (<http://creativecommons.org/licenses/by/4.0/>).